

Efficient Deep Speech Understanding at the Edge

Rongxiang Wang
University of Virginia
waq9hw@virginia.edu

ABSTRACT

Contemporary Speech Understanding (SU) involves a sophisticated pipeline: capturing real-time voice input, the pipeline encompasses a deep neural network with an encoder-decoder architecture enhanced by beam search. This network periodically assesses attention and Connectionist Temporal Classification (CTC) scores in its autoregressive output.

This paper aims to enhance SU performance on edge devices with limited resources. It pursues two intertwined goals: accelerating on-device execution and efficiently handling inputs that surpass the on-device model's capacity. While these objectives are well-established, we introduce innovative solutions that specifically address SU's distinctive challenges:

- (1) *Late contextualization*: Enables the parallel execution of a model's attentive encoder during input ingestion.
- (2) *Pilot decoding*: Alleviates temporal load imbalances.
- (3) *Autoregression offramps*: Facilitate offloading decisions based on partial output sequences. Fig: Intro

Our techniques seamlessly integrate with existing SU models, pipelines, and frameworks, allowing for independent or combined application. Together, they constitute a hybrid solution for edge SU, exemplified by our prototype, *XYZ*. Evaluated on platforms equipped with 6-8 Arm cores, our system achieves State-of-the-Art (SOTA) accuracy, reducing end-to-end latency by 2x and halving offloading requirements.

ACM Reference Format:

Rongxiang Wang and Felix Xiaozhu Lin. 2023. Efficient Deep Speech Understanding at the Edge. In *Proceedings of ACM Conference (Conference'17)*. ACM, New York, NY, USA, 13 pages. <https://doi.org/10.1145/nnnnnnnnnnnnnnnn>

1 INTRODUCTION

Speech is a pervasive user interface for mobile and embedded devices. At its core are two speech understanding (SU) tasks. Automatic speech recognition (ASR) transcribes voice to a sentence [39]; spoken language understanding (SLU) maps voice to a structured intent, such as {SCENARIO: Calendar, ACTION: Create_entry} [9].

Modern SU: autoregression with beam search Modern SU runs a deep, encoder-decoder model [8] as shown in Figure 1. Ingesting an utterance waveform, the model comprises a neural encoder,

Permission to make digital or hard copies of all or part of this work for personal or classroom use is granted without fee provided that copies are not made or distributed for profit or commercial advantage and that copies bear this notice and the full citation on the first page. Copyrights for components of this work owned by others than ACM must be honored. Abstracting with credit is permitted. To copy otherwise, or republish, to post on servers or to redistribute to lists, requires prior specific permission and/or a fee. Request permissions from permissions@acm.org.

Conference'17, July 2017, Washington, DC, USA

© 2023 Association for Computing Machinery.

ACM ISBN 978-x-xxxx-xxxx-x/YY/MM...\$15.00

<https://doi.org/10.1145/nnnnnnnnnnnnnnnn>

Felix Xiaozhu Lin
University of Virginia
felixlin@virginia.edu

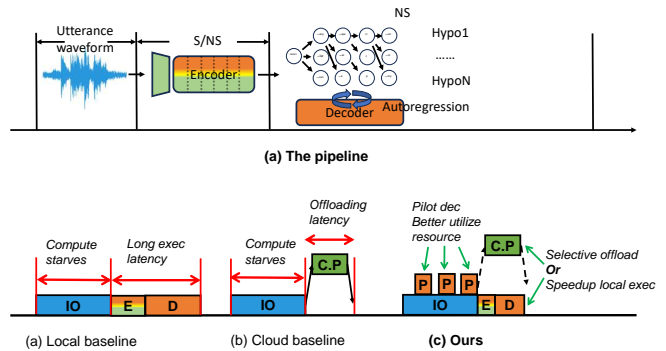


Figure 1: Comparison of different speech processing scheme. Our method achieve low latency for local execution, also help achieve higher accuracy by selectively offload part of the data to cloud. E: encoding, D: Decoding, C.P: Cloud processing, P: Pilot inference

which captures dependency among sound units, and a neural decoder, which generates a sequence of tokens as words or sub-words. This generation process is autoregressive: to produce a token, the decoder takes as input all the latent units produced by the encoder, as well as the output tokens it produces so far. To cope with noisy utterances, SU runs multiple such decoding processes concurrently, each generating a candidate output sequence (called a hypothesis). Scoring all hypotheses with attention and CTC (connectionist temporal classification) [34], SU picks the best one as the final output. Thanks to such an encoder-decoder architecture wrapped in beam search, modern SU can understand sophisticated utterances (e.g. “I need to turn on light in bedroom”) [7] rather than simple commands (e.g. “light on”).

Deep SU models are resource-hungry. The ones with satisfactory accuracy often require GBs of memory and tens of GFLOPs per input second [5]; even after being compressed to fit in embedded devices, the resultant models can take more than 10 seconds to process an input (see Section 7 for details). Seeing the constraints, many embedded devices choose to offload all voice inputs to the cloud [2], which, however, raises concerns on high cost [4] [3][1], privacy [31], latency [23], and availability.

Problem & approach This paper sets to accelerate deep SU on resource-constrained embedded devices¹. We present an on-device SU engine that integrates a local execution path and an offloading path; the former is optimized to reduce on-device delays and the latter selectively offloads the inputs beyond the device capacity, ensuring high overall accuracy. While our approach is reminiscent of numerous ML systems for vision and NLP [22, 32, 38], our design specifically addresses unique challenges from SU.

¹Referred to as “devices” for simplicity, will be defined in Section 2

1.1 The local execution path

Challenge: temporal load imbalance We identify a key inefficiency in SU execution: poor resource utilization during the ingestion time. While a typical utterance spans at least several seconds, the compute is mostly idle during the ingestion period, because most of an encoder-decoder model is to be executed over a complete input, thanks to the all-to-all attention. Yet, as soon as the ingestion completes, a surge of workload – encoding and then decoding – emerges, which incurs long delays directly perceived by the user.

Naively feeding truncated (i.e. yet to complete) utterances to an SU model result in significant errors, as the model has been trained on, and therefore expects, complete utterances. While some SU models are designed to process streaming inputs [17], they often make significant compromise on accuracy [20], as will be discussed in Section 8.

In summary, we need to utilize ingestion-time resources to accelerate the expensive processing that can only start after the ingestion.

Our design

Our first technique, called late contextualization, refactors an SU model so that most of *encoding* layers can execute in parallel to ingestion. Rather than computing all-to-all attention at each encoding layer, the bottom layers (closer to the input) compute only convolution, whereas the few top layers compute attention.

Our second technique is called pilot inference: during ingestion, SU periodically encodes and decodes the incomplete input accumulated so far. As mentioned above, inference on a truncated utterance will result in substantial errors, particularly near the sequence’s end. Yet, our key insight is that the pilot inference’s *intermediate state* can assist the subsequent full inference (i.e. executed over the complete input) in multiple ways: (1) beam collapse: the full inference only needs to verify its beam search path against the path in the pilot decoding, and only falls back to full beam search in case of path divergence; (2) early search termination: extrapolating the output length of pilot inference, the full inference predicts the final output length and prunes any astray search paths; (3) CTC leap: approximating the CTC prefix scoring [34] with the scores already computed in pilot inference.

A nice property of pilot inference is being incremental. As shown in Figure 1, the $(i+1)$ -th inference instance reuses of the state from the i -th instance, in the same way as the full inference reuses the last pilot inference instance. In this way, the total cost of pilot inference is amortized over the duration of ingestion, and scales gracefully with the input length.

Pilot inference is related to speculative execution for language models [16], however with a key difference: while the latter optimizes inference on complete inputs, PI processes successive *incomplete* inputs, which entails different challenges and techniques. Section 8 presents a detailed comparison.

1.2 The offloading path

Challenge: Offramps for autoregression

To decide whether to offload an input x , the device assess how likely the on-device inference of x would yield a sufficiently accurate answer. Often, such an assessment of *confidence* is based on

shallow processing of x , which is referred to as *offramps* in prior work. Existing offramp designs typically evaluate confidence as an ML model’s prediction entropy [36, 41]. For SU however, existing offramps mismatch for two reasons.

First is the *confidence measure*. Unlike common classification tasks which evaluate a model’s layers sequentially, SU’s output generation is both concurrent and iterative: it produces multiple hypotheses of probabilistic tokens; to produce each token it evaluates all the decoder layers. To complicate the issue, one hypothesis often comprises tokens that have drastically different probabilities. It was unclear how to derive one confidence score out of such a generation process.

Second is *timing*. Given an input, offramp represents a one-shot decision that can be taken at various times throughout the SU pipeline shown in Figure 1. While by deferring the decision the offramp would have more input information to reliably measure the model confidence, it also incurs non-trivial on-device delays should the offramp eventually decide to offload. The timing therefore hinges on non-trivial tradeoffs between offramp selectivity and overhead.

Design 2: Offramps for autoregression

The device evaluates its offloading decision as soon as it finishes ingestion, based on the last pilot sequence’s perplexity score [14]. Doing so strikes a sweet-spot tradeoff between the offramp’s selectivity and overhead: (1) the pilot sequence’s perplexity is close to the perplexity of the full decoding; (2) The device avoids delaying the offloading decision until the slow full decoding. Note that this is the earliest moment the device can offload: offloading *before* the ingestion completes, does not reduce the offloading delay: as an input utterance is as small as tens of KB, the upload is bound by network latency under typical network conditions; another network round trip is nevertheless needed.

1.3 Results and contributions

We implement the above ideas in a system called XYZ, atop two embedded platforms, with 6 or 8 Arm64 cores respectively. We test XYZ on SLURP [7], a challenging speech benchmark comprising 102 hours of speech. On both ASR and SLU tasks, XYZ delivers strong accuracies with end-to-end latencies as low as 100s of ms. XYZ’s on-device execution incurs 2x lower latency as compared to popular, efficiency-optimized models running on device. Augmented with offloading, XYZ’s hybrid execution offers much higher accuracy than the on-device models at similar or low latency; the hybrid execution offers close-to-gold accuracy (only 1% in IC lower than SOTA), while incurring 47%-53% lower offloading compared to an all-offloading approach.

Contributions Towards deep SU on embedded devices, we contribute:

- An encoder-decoder model architecture (convolution on bottom layers; attention on top layers) so that it suits early offloading on streaming (partial) inputs.
- Pilot inference, a novel way to address resource underutilization during ingestion. Note that pilot decoding, as a generic optimization technique, can be applied to other models without modifying their architectures.

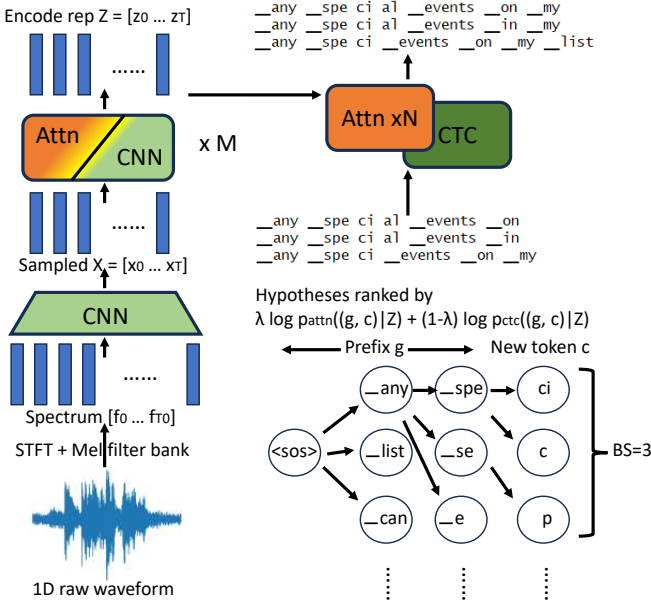


Figure 2: The vanilla speech understanding pipeline. The input of SU tasks, an 1D raw waveform of the audio, will first go through STFT+Mel filter bank to get spectrum, then processed by encoder to get intermediate encode representation, and finally decoded in an autoregressive fashion by hybrid transformer/CTC decoder coupled with beam search method

- An offramp design that assesses model confidence in generative, autoregressive output. This is the first mechanism for offloading generative tasks, to the best of our knowledge.

2 MOTIVATIONS

2.1 The system model for deep SU at the edge

The SU tasks today happen at the mobile devices on the edge. These devices usually have several CPU cores (4 - 8) and around 100MB of memory budget for each application [18][19]. Wireless or 5G network connection is usually available for the communication with the cloud service provider. During the SU tasks, the user speak to the device and expect low latency after they finish speaking. The system can detect the beginning and termination of the speech accurately[21][24].

2.2 A primer on speech understanding

Deep SU at the edge: an important, unsolved task The SU task is still remain unsolved. Current methods can attain satisfactory accuracy on simple datasets such as LibriSpeech[26]. The WER (word error rate) can be as low as 4%, outperform human performance. However, as mentioned in previous study[12], there is usually a large gap between benchmark accuracy and the accuracy in real life. This also reflect on accuracy result on SLURP dataset, which is a dataset closer to real-life speech. Achieving higher accuracy requires larger model, but hardware limitations makes the model execution infeasible.

The typical speech processing system The state-of-the-art speech processing system, shown in Figure 2, utilizes a transformer-based encoder-decoder model for inference, which involves an autoregressive beam search process [11] [27] [6].

The encoder and encoding process Typically, the encoder in an SU model consists of multiple layers that combine CNN and transformer elements. This design can be found in models like Conformer[11], Branchformer[27], Wav2vec[6], HUBERT[13], and others. During operation, as shown in Figure 2 left part, the 1-D speech data will be broke in to frames and undergoes STFT and Mel-filter bank methods to create a 2D spectrum that have $f_1 \dots f_{T_o}$, each f_i is the processed frequency component of that time frame. The 2D spectrum $[f_1, \dots, f_{T_o}]$ is then processed by a few convolutional layers for downsampling, $X = x_1, \dots, x_T$ is get from $X = \text{subsampling}([f_1, \dots, f_{T_o}])$. The X is subsequently passes through multiple encoder layers that include both convolutional and transformer component and get the latent speech representation Z among the same time frames z_1, \dots, z_T like $X, Z = \text{encoders}(X)$. This entire encoding process is a one-pass operation, providing an intermediate representation of the speech signal framewise with a specific dimension.

The decoder and beam search decoding The decoder typically includes a transformer decoder and a CTC decoder. The rationale is that the transformer decoder comprises several transformer layers excel in maintaining language consistency, while the CTC decoder is a linear layer primarily focused on audio features.

The generation of the final transcript involves an autoregressive beam search process as shown in Figure 2 right part, with tokens generated one by one. The beam search employs a specific beam width (k), maintaining k developing hypotheses during the decoding process. In decoding, the CTC decoder first calculates posterior token probabilities $p(z_i = c|Z)$ for each frame z_i of the encoder output. The beam search is shown in the Figure 2 lower right part. Beginning with the "<sos>" (start of the sentence) token, the transformer decoder calculates the next token c 's posterior probabilities based on current partial hypothesis g and speech latent representation and get $p_{attn}(c|g, Z)$, combine with the previous token probability we have $p_{attn}((g, c)|Z)$. The CTC prefix scorer, utilizing dynamic programming methods, further calculates CTC prefix probabilities $p_{ctc}((g, c, \dots)|Z)$ based on newly developed hypotheses (g, c) and the CTC framewise output $p(z_i = c|Z)$. The best K hypotheses with highest $\lambda \log p_{attn}((g, c)|Z) + (1 - \lambda) \log p_{ctc}((g, c, \dots)|Z)$ are retained in the beam for the subsequent rounds of decoding, based on a weighted sum of probabilities from the transformer decoder and CTC prefix scorer. The decoding process concludes when the completed hypothesis significantly outperforms the developing hypotheses, as described in [34].

2.3 Observations & challenges

The following unique characteristics of raise challenges.

Observation: streaming, steady ingestion. The execution timeline for speech understanding tasks, particularly those dealing with streaming audio data, significantly differs from vision and NLP tasks due to the nature of the data. Data ingestion in speech tasks typically takes a relatively long time (e.g., LibriSpeech at 5 seconds, SLURP at 3 seconds on average). After completing full data ingestion, the

data goes through the one-pass encoding and autoregressive beam search decoding, token by token, as previously mentioned. In contrast to vision and NLP tasks, which usually have the entire dataset readily available from the start, the SU system must wait for speech ingestion to finish. During ingestion, I/O operations are active while the CPU remains idle.

Observation: input context matters to accuracy The information in the input audio is distributed throughout its entire duration, with the entirety of the audio serving as the context for each individual part. While waiting for data ingestion may seem to hinder resource efficiency, it is a necessity for attention models. The all-to-all attention mechanism in transformer-based models is the key to their superiority in NLP and speech-related tasks. This mechanism leverages contextual information from the complete dataset to generate results with better language consistency. As shown in prior work [8] [27] [11], any portion of the output should take into account the whole input (i.e. the context). For instance, in the input "X Y Z" the accurate prediction of X (or X'?) depends on Z. Here are some real-life example: in context with with time related phrase, words like "calendar" or "reminder" is more likely to occur, like "set reminder for xx event at 4pm" or "check my calendar to see if I have appointment tomorrow". Partial input data with incomplete context can significantly impair the model's decoding accuracy, forcing the model to wait until ingestion is complete. [28]

Challenge 1: Under utilized resources during ingestion time As previously mentioned, there is an imbalance in resource utilization throughout the operation of the SU system. The CPU remains idle during ingestion, while it becomes busy during the time-consuming encoding and decoding processes. This has motivated us to explore opportunities for offloading a portion of the encoding and decoding computations during the ingestion period.

Observation: complex decoding with numerous neural function evaluations (NFEs) In SU tasks, Hybrid CTC/Attention beam search decoding is widely adopted. The decoding is based on beam search, and in each round of beam search, hypotheses are scored by both the transformer and CTC prefix scorer. This hybrid scoring scheme is unique to speech, where the transformer contributes more to language consistency, while CTC exploits the acoustic features, enabling the model to achieve decent accuracy in a relatively small size.

The hybrid CTC/attention beam search decoding exhibits significant computational complexity, entailing trade-offs between accuracy and latency for both beam size N and beam search length L .

For beam size N , abstracting the transformer scorer and CTC prefix scorer as NFE (Neural Function Evaluation) in each beam search round yields a complexity of $O(N \times \text{NFE})$. Larger beam sizes result in linear increases in computation and latency in CPU-only processing scenarios. Given the nature of beam search, most hypotheses in the search are discarded. Regarding beam search length L , with a fixed beam size, the overall computation complexity is $O(L \times \text{NFE})$. In the default setting, the current average beam search length is ~ 18 , while the average transcript length is ~ 11 , indicating clear redundancy. Moreover, the CTC prefix scorer computation, driven by a poorly parallelized dynamic programming algorithm across all time frames in each NFE term, sometimes incurs higher

latency than the transformer score NFE, contributing to decoding challenges.

Challenge 2: Long decoding latency b/c of the above reasons, the decoding is slow on typical edge devices. As we will show in section 7, on cpu, the latency is 0.75 s (for a typical 3 s input). In particular, because the workload is irregular, it does not benefit much from typical mobile GPUs. Our experiment on Nvidia's Ampere mobile GPUs show it is even slower on GPU than on CPUs. It is likely due to GPU is under utilized. experiments on embedded devices (6CB in Table 1) shows that GPU processing take even longer time (GPU 1.2 s vs CPU 0.75 s).

3 XYZ OVERVIEW

3.1 The on-device model

Encoder: late contextualization XYZ features a novel encoder designed shown in Figure 3a. and b.(①) which separate the streaming convolutional part and non-streaming transformer part to enable more than half of the computation to get done during data ingestion.

As shown in Figure 3a., our model is motivated by the Branchformer [27], which have parallel convolutional and transformer blocks in each layer for local and contextual feature extraction. The learned weight shows the redundancy in the model. Our model keeps the blocks that have higher weight and rearrange them to make the convolutional layers which enable streaming processing at the beginning to hide the computation latency into the ingestion time.

Decoder As shown in Figure 3, XYZ has two versions of the decoder for pilot inference (②) and full inference. By default, the pilot decoder shares the same structure and weights with the full decoder but has a smaller beam size.

The training details can be found in Section 6

3.2 The operations

As shown in Figure 3b., XYZ ingests segments of voice input $x_{1..n}$. On each segment, XYZ executes the cgMLP (convolutional) encoder layers per-segment results y_i that can be combined later. Periodically, the device executes pilot inference (②) with idle compute resources: sending the accumulated segments $\{z'_{i=1..k}\}$ to the attentive encoding layers to get $\{z_{i=1..k}\}$, followed by the decoding process that generates a sequence of tentative tokens, which we refer to as a "pilot output". Over the course of ingesting an input, XYZ may execute pilot inference multiple times, each time on an increasingly longer input. The execution of pilot inferences is incremental: each inference reuses computation of the previous instances. The frequency fo pilot inferences is a configuration parameter to be evaluated experimentally. Essentially, this periodical pilot inference tries to extract as much information as possible from the partial inputs, *during* the ingestion. This information benefits the subsequent execution in two ways. For local execution, the information aids in speeding up decoding. For hybrid execution, the information contributes to local confidence estimation and the selection of the execution path.

Once the ingestion is over (detected with auxiliary means as in prior work. e.g pause [21]), the device evaluates the offloading

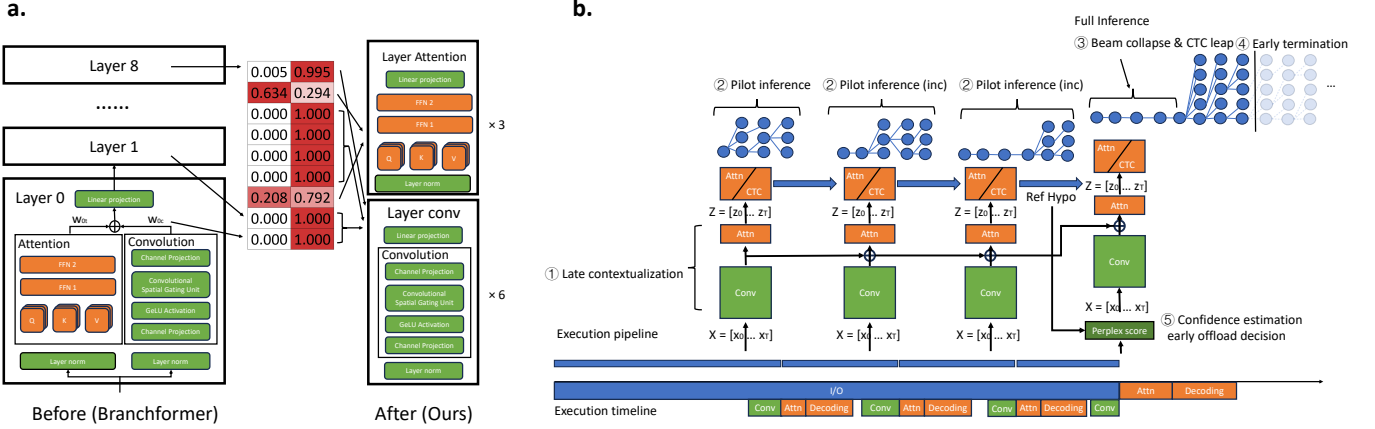


Figure 3: a. Compared to popular encoder-decoder SU models (left), our model (right) shifts much of the encoding computation to bottom layers, allowing them to be executed in a streaming fashion during ingestion. b. Execution pipeline of XYZ. Our system conduct pilot decoding periodically on partial input, and use the pilot decoding result to speedup the final decoding

fig:pl

decision immediately (and aborts the ongoing pilot inference, if any) by computing the confidence score of the most recent pilot output. By doing so, the decision can be made without waiting for inference on the compute input $\{x_{i=1..n}\}$; since this pilot inference is based on an input with length closest to the complete input, its confidence is close to the full length decoding confidence.

If confidence is low, XYZ offloads the input as waveform and waits for results; otherwise, it finishes encoding $\{x_{i=1..n}\}$ and executes the full decoding over $\{z_{i=1..n}\}$. Although the device cannot directly emit the pilot output because of the latter's high errors, the decoding benefits from pilot output in crucial ways: to reduce the beam search width, to approximate the CTC prefix scores, and to help with the beam search early termination.

3.3 Applicability

Our key techniques can be applied independently or in combination to existing SU deployment. (1) Late contextualization and pilot inference both speed up local execution; they can be applied separately to existing models. Specifically, pilot inference can be applied to existing unmodified models, such as branchformer, HuBERT, etc. Notably, it is compatible with both CTC decoding (classic), attention decoding (modern, such as in Whisper [29]), or a hybrid one, as we will show in Section 7. We will show this in evaluation. (2) Offramps optimizes offloading decisions; it can be applied to existing local models (without our enhancement) in order to form a hybrid solution. The caveat is that the decision has to be evaluated on full decoding sequence, which incurs extra delays as compared to our system.

Our techniques require light modifications of the existing SU implementations. It does not require to develop new ML operators. To this end, our techniques apply to the cases where SU has a CPU backend or GPU backend. Late contextualization requires to train a new model architecture (which involves light effort, see Section 4.1); the model can run atop existing ML libraries such as ONNX runtime and espnet. Pilot inference and offramps modify the SU pipeline logic, which is often implemented in Python code on CPU.

4 THE LOCAL EXECUTION PATH

This section focuses on pilot inference for local execution.

4.1 The mechanisms

Pilot inference works periodically on partial data as shown in Figure 3 (②). XYZ refrains from performing pilot inference on excessively short data as it is hard to generate meaningful result with too short partial data. During data ingestion starting from T_s , the system conducts pilot inference on partial data periodically with a pre-defined granularity of δt_s , intended to complete within δt_s . In each round of pilot inference, the system utilizes the same encoder and the pilot decoder to engage in beam search inference with a beam size of k . Supposing the pilot inference is conducted on data for $T + n\delta t_s$, the results cover the full data that have length range between $[T + (n+1)\delta t_s, T + (n+2)\delta t_s]$. To manage the runtime of pilot inference, a token limit of 1 tokens is set. Following the decoding of 1 tokens, the hypothesis with the highest probability (highest score) is chosen as the reference hypothesis for local execution or hybrid execution path decisions. The reference hypothesis, denoted as $y_{p1:n} = (y_{p1}, \dots, y_{pn})$, offers the potential to accelerate the full inference process from multiple perspectives mentioned in the next few subsections.

Hyperparameters Several key parameters in pilot inference require pre-operation definition. These parameters include granularity δt , beam size k , and the maximum token length for beam search inference, denoted as l . These hyperparameters are determined through heuristic methods based on experimental experience. The granularity needs to be established initially. Typically, the system anticipates that the longest partial data covers at least 70% of the full-length data. To achieve this, the granularity is expected to satisfy $d < 0.2l$. It's important to note that the granularity doesn't have to remain a fixed number throughout system operation. As data lengthens, the pilot inference take longer time as shown in Figure 3 (②) comparing the different pilot inference, the granularity can also expand. The beam size for pilot inference is set at 60% of the beam size used for full decoding to ensure lightweight pilot inference while maintaining fidelity. The inference length is determined based on

decoding behavior profiles and average inference length. If the average inference length is l_{full} , XYZ sets l to be $0.7 * l_{full}$.

Incremental execution The pilot inference based full decoding acceleration techniques (which will be elaborated in the following sub-sections) can also be adopted in the pilot inference execution. More specifically, the reference based beam collapse can be adopted in the pilot inference. In our system, as shown in Figure 3 (②), from the second pilot inference, each pilot inference can take reference hypothesis from the previous pilot inference and perform strict beam size reduction in the pilot beam search procedure. Incremental decoding is critical for pilot inference runtime reduction.

4.2 Optimization: beam collapse

Assumption One basic assumption on full decoding is that most tokens of the full transcript should be the best token in the beam search decoding process at the corresponding round. For the beginning part of the transcript, the reference transcript from pilot inference should share most of the tokens the same with the final transcript. **What we do** Base on this assumption, during full inference, starting from the first token, in each inference round before predicting the next token probability using the transformer and CTC prefix scorer, the system attempts to validate the reference hypothesis. It initially checks the latest token, y_i . If $y_i = y_{pi}$, the token is validated, and the system retains only the best hypothesis for the subsequent token calculation in this round. **Complexity reduction** This verification reduces the computational load for predicting the next token to 1 / beam size, also reduces required NFE to 1/N. **Why such approximation is acceptable** The approximation is reasonable because of two point: the reference result is from pilot inference (which has accuracy that does not degrade that much) works on most part of the data by design. The verification step also partially secures the inference not to be deviated by the potential wrong part in the reference transcript.

4.3 Optimization: early termination of search

Assumption Another assumption on full decoding is that the reference inference results can reflect the final transcript length, the token number grows proportionally as time grows. **What we do** The system predicts the final inference length using three key parameters: the length of the partial data, $l_{partial}$ obtained in the latest pilot inference; the full data length, l_{full} ; and the token count of the reference hypothesis, n_p . The calculation for the full inference length is expressed as $n = l_{full}/l_{partial} * n_p + C$. This calculation assumes a naive distribution of tokens across time. Here, C represents a tunable constant that provides the full inference with a slight buffer. During the full inference, when the full inference reaches the predicted length n , if there are terminated hypotheses, the system terminates the beam search inference. Alternatively, the system continues inference until at least one hypothesis ends before terminating the process. **Complexity reduction** Assume the vanilla beam search length is l_v , the early termination can save $(l_v - n)$ NFE calculation. **Why such approximation is acceptable** The approximation works well because the tokens distribute evenly among time statistically. The loose factor C can also help to decrease the deletion error that introduced by too aggressive early termination.

4.4 Optimization: CTC leap (prefix scoring speedup)

Assumption An basic assumption of CTC prefix scoring is that the CTC prefix score calculation in pilot inference could be reuse in the full inference. In each prefix ctc score calculation, the pilot inference calculate the prefix probability among all the partial audio time frame through a dynamic programming algorithm that loop from the beginning time frame to the end time frame and get $p_{ctc}(h|T_{pilot})$. The full inference ctc score calculation, by default also need to loop from beginning time frame to the end frame of full audio, in which the calculation from starting frame to T_{pilot} frame is almost identical. Thus with the pilot inference result the system can skip the beginning part of the calculation for each prefix and reuse the corresponding part in pilot inference to get the $p_{ctc}(h|T)$ only loop from T_{pilot} to T . Conceptually, the system separate the $p_{ctc}(h|T)$ calculation into $p_{ctc}(h|T_{pilot}) + p_{ctc}(h|[T_{pilot}, T])$ and only calculate the later part.

What we do The system also includes CTC prefix scoring speedup when working with hybrid CTC/transformer beam search decoding. The CTC prefix scoring works alongside the transformer decoder in the hybrid CTC/transformer beam search decoding process. It calculates the probabilities for prefixes (hypotheses that have not reached the end), which are then combined with the probabilities obtained from the transformer decoder to form the overall probability. This calculation is based on a dynamic programming algorithm. For a prefix $h = (g, c)$, where g represents the previous hypothesis and c is the next token, the system calculates two forward probability arrays: $r_{[0 \dots T]}^b(h)$ and $r_{[0 \dots T]}^{nb}(h)$. These arrays are based on the forward probability arrays $r_{[0 \dots T]}^b(g)$ and $r_{[0 \dots T]}^{nb}(g)$, as well as the CTC posterior probability matrix $p(z_t = c|X)$. This matrix is calculated by the CTC linear layer and the encoder output X . During the calculation of forward probabilities, for a given t , $r_{[t]}^b(h)$ and $r_{[t]}^{nb}(h)$ are calculated based on $r_{[t-1]}^{nb}(h)$, $r_{[t-1]}^b(h)$, $r_{[t-1]}^{nb}(g)$, and $r_{[t-1]}^b(g)$. Hence, this calculation requires looping from 0 to T . With the pilot inference results, the system can skip the calculation of $r_{[0 \dots p*T_{pilot}]}^{nb}(h)$ and $r_{[0 \dots p*T_{pilot}]}^b(h)$. $p \in [0.5, 1]$ is a predefined factor that help discard the final part of pilot CTC prefix scoring result. During the pilot inference, the system records $r_{[0 \dots T_{pilot}]}^{nb}$ and $r_{[0 \dots T_{pilot}]}^b$ of each partial hypothesis in a list. When transitioning to full inference, if the pilot inference token is verified, the system can adopt the speedup during the CTC prefix calculation. The calculation of $r_{[0 \dots T]}^b(h)$ and $r_{[0 \dots T]}^{nb}(h)$ will start by assigning $r_{[0 \dots p*T_{pilot}]}^b(h)$ and $r_{[0 \dots p*T_{pilot}]}^{nb}(h)$ to the corresponding calculation results from the pilot inference. Subsequently, it calculates $r_{[p*T_{pilot} \dots T]}^b(h)$ and $r_{[p*T_{pilot} \dots T]}^{nb}(h)$ as usual. **Complexity reduction** By implementing this process, when the speedup requirement is met (pilot inference token is verified), the CTC prefix probability calculation in this round can be saved by $p*T_{pilot}/T*NFE_{CTC}$. **Why such approximation is acceptable** The posterior probability matrix of pilot inference which shapes $[tokens, T_{pilot}]$ should be almost the same with the $[0 : T_{pilot}]$ slice in the one in the full inference which shapes $[tokens, T]$, or at least most part should have the similar value. Besides, the dynamic programming algorithm in

$p_{ctc}(h|T_{pilot})$ calculation only involve previous time frame, so it should be the same in both pilot inference and full inference.

4.5 Implications of approximation

Approximate execution is common to SU and more general autoregressive system like LLM, because the whole thing is statistically in nature; and people often make approximate at their discretion, as long as the approximation can be empirically validated. The speculative decoding technique in [16] also involves tentative hypothesis validation. The beam search end estimation technique in [15] introduce tunable parameter "patience factor" to help tune the beam search length. The truncate CTC prefix scoring in [25] estimate the CTC prefix alignment with time frame to save part of the computation. Different from these method, our system can better work on these estimation with the help of reference result from pilot inference.

5 THE OFFLOADING PATH

While the above designs accelerate the local execution, the SU task accuracy is nevertheless bound by the model size on the device. To deliver SOTA accuracy, we further augment the SU pipeline with cloud execution. The key challenges are twofold. (1) The device should estimate confidence (as the offloading criteria). Existing method[36] used in classification tasks cannot be directly applied to the generative SU task. It is because it works with the BERT style encoder, only take first frame of the output for classification and cannot take the full input into consideration. (2) The device should do so without delaying the local processing. It cannot, for example, simply evaluate the decision *after* full inference, as this would result in extended local decoding times for all inputs. It also cannot offload *prior to* ingestion completion: as each voice input is typically tens of KB to ~300 KB for speech less than 10 s, the offloading is bound by network round trips (RTTs); the device would still need one RTT to offload the whole input, after the ingestion completes.

Confidence estimation *Perplexing Score-Based Approach* The perplexing score is derived from the reciprocal of the average probability of all tokens in the hypothesis, calculated by $\exp(-\frac{1}{l} \sum_{i=0}^l \log(p(x_i|x_{<i}))$. A high perplexing score indicates low confidence of the local model with the data. The system sets different thresholds for the perplexing score and offloads data that surpasses these thresholds.

RNN-Based Approach During beam search, we further gather the probability of each token in the hypothesis. This fine-grained probability information better represents the local confidence in the data. Different patterns in the token probability sequence may signify various meanings. For instance, sequences of low-probability tokens often imply a lack of model confidence in the semantic correctness of an entire output span. Conversely, if such tokens are scattered, it could be attributed to acoustic noise while the output remains mostly correct. Defining rules manually can be challenging, so we adopt a learning approach: constructing a lightweight BiLSTM model to predict whether the SU (System Understood) result accuracy is lower than a certain threshold p'' . To achieve this, we partition the development set data into two classes based on their accuracy and the threshold ' p' , and then train the BiLSTM model. The model's output on the test data serves a similar role as the perplexing score mentioned earlier.

CNN-Based Approach The intermediate results from the encoder contain rich information about the data but possess significantly higher dimensions compared to the token probability sequence. To address this, we propose a CNN-based approach to assist in downsampling the intermediate results. Similar to the RNN-based approach, we train the CNN to predict the SU accuracy. This model is also trained on the development set. The model's output on test data serves a similar function to the perplexing score. It's noteworthy that during the design of the CNN network, we observed that CNNs typically require a larger number of weights compared to the RNN approach. This issue of model size makes it less practical.

Decision timing The XYZ makes the offloading decision precisely when the data ingestion is completed, along with the pilot inference result. This is shown in Figure 3 Both the perplexing score method and the BiLSTM method require post-decoding results. However, if the system performs confidence estimation after the full local execution, the offloaded data will also suffer from local decoding latency. To circumvent this, the system executes the aforementioned methods on the latest pilot inference result, , i.e. the 3rd pilot inference in Figure 3 enabling the system to make the execution path decision simultaneously with the completion of data ingestion. This approach is founded on the assumption that the partial data in the pilot inference can reflect corresponding information in the full-length data.

6 IMPLEMENTATION

We implemented XYZ using 4K SLOC in Python, built upon the renowned speech toolkit ESPnet.

Model training details The model training envolves multiple steps. To train our model, we first configure and train an example branchformer model base on the memory and latency budget. In the experiment case, 9 layers of encoder and 1 layer of decoder. To construct XYZ's model, assume there are k transformer blocks with weights exceeding a threshold h in the trained branchformer encoder, we design the encoder with $N-k-1$ CNN layers followed by $k+1$ transformer layers. In the experiment, we get $2+1$ transformer and $9-2-1$ CNN layers. This design is then trained from scratch on the same dataset, with the same decoder design branchformer model has. The comparison with the branchformer encoder is illustrated in Figure 3a.

Operation details During system operation on the SLURP dataset, we set the shortest partial data for pilot inference at 1.5 seconds. This granularity is determined based on hardware specifications, tested across intervals of 0.5s, 0.7s, 1s, and 2s. The pilot beam size is established at 3, which is 60% of the full inference beam size of 5. The limit for pilot inference tokens is set to 15. For full inference, the system selects the best hypothesis with the highest probability among finished and running hypotheses from the last pilot inference. The length prediction C is set to be 5. To optimize CTC prefix scoring, ESPnet introduces a pre-beam to reduce possible prefix calculations. In the pilot inference, the pre-beam size is set at 10, while the full inference selects the 10 best tokens from the transformer. If there are 7 or more tokens in the intersection of the pilot and full set, the CTC prefix scoring speedup is applied to these 7 tokens. If not, the speedup is disregarded, and the pre-beam size falls back to

7, choosing the 7 best tokens from the transformer decoder to do the CTC prefix scoring.

Hybrid execution details For hybrid execution and offloading decision-making, in the perplexing score-based method, we calculate the perplexing score based on the reference result from the pilot inference. Regarding the BiLSTM and CNN-based methods, we utilize the full development set in SLURP as the training set for the BiLSTM and CNN models. The CNN approach employs a CNN model that takes the encoder’s intermediate output as input. The CNN model has two convolutional layers and two fully connected layers, with 192.5 M parameters. The LSTM approach employs a BiLSTM model that takes CTC prefix probability and transformer token-wise probability of the reference result as the input. The LSTM model we adopted is a 1-layer BiLSTM model with 11.1k parameters. The training task is defined as a binary classification task, where a local execution WER > 0.1 is labeled as 1, and otherwise as 0. During operation, the BiLSTM and CNN process the respective input and provide predictions, representing the probability of the data having a WER > 0.1 as a float number between 0 and 1. Further, we set thresholds for different offloading accuracy targets.

7 EVALUATION

We answer the following questions:

- Can XYZ reduce latency with competitive accuracy?
- XYZ’s local path: what is its efficacy?
- XYZ’s offloading path: what is its efficacy?

7.1 Methodology

Test platforms As shown in [Table 1](#), we test on two embedded boards: 6CB with an efficiency-oriented SoC with six cores, whereas 8CB with a performance-oriented SoC with eight cores. Our experiments focus on CPUs, though our idea applies to GPUs as well.

We run the cloud runtime on platform an x86/NVidia machine and measure accuracy. To better estimate the cloud offloading delay, we measure Microsoft’s speech service [\[2\]](#): we invoke the Azure APIs to offload waveforms and record each waveform’s end-to-end wall time. Our measurement runs from the US east coast and invokes datacenters on the east coast. For each input, we repeat the test on enterprise WiFi (bandwidth in 100s of MB and RTT in ms) and on 5G cellular networks, and take the average. Note that we do *not* use Azure speech for accuracy evaluation, as we often find its accuracy inferior to the SOTA model (2 pass SLU [\[5\]](#)) used by us.

Dataset and model training We run our experiments on SLURP [\[7\]](#) as summarized in [Table 2](#). Comprising 101.8 hours of speech, SLURP’s utterances are complex and closer to daily human speech (e.g. “within the past three months how many meetings did i have with mr richards”), as opposed to short commands (e.g. “light on”) in many other datasets. Of all 141,530 utterances, we use 119,880 (85%) for training and the rest for develop set and test set. The accuracy and latency are reported from the test set data range from 2s to 6s, which covers 70% of the test set.

Metrics We follow the common practice. **Accuracy**. For ASR, we report word error rate (WER): the discrepancy between the model output and the ground truth transcript, defined as count of errors

Platform	Compute resource	GFLOPs/s
6CB	6-core Arm Cortex-A78AE 64-bit CPU 1.5GHz	14.9
8CB	8-core NVIDIA Carmel Arm 64-bit CPU 2.2GHz	30.8

Table 1: Embedded platforms used in evaluation

	Train set	Develop set	Test set	Overall
Speaker number	167	137	142	177
Audio file	119880	8690	13078	141648
Total audio len	84.7 h	6.9 h	10.2 h	101.8 h
Audio len stats	2.5±1.1 s	2.9±1.2 s	2.8±1.3 s	2.6±1.1 s
Token num stats	11.4±6.1	11.5±6.4	11.3±6.7	11.4±6.2

Table 2: Overview of SLURP dataset, an important SLU dataset.

(substitutions, deletions, insertions) normalized by the sentence length. For SLU, we report the intent classification accuracy (IC).

Latency. (1) We report user-perceive latency [\[39\]](#): the elapsed time from a user completing her utterance to the system emitting the complete SU result. (2) We further report the real time factor (RTF): the user-perceived latency normalized by the input utterance’s duration.

Baselines We compare the following designs.

- *OnDevice*: SU completely runs on device, for which we test a wide selection of model architectures: Conformer [\[11\]](#), Branchformer [\[27\]](#), and CNN-RNNT [\[40\]](#). Note that CNN-RNNT is streaming, with 640ms chunks as in prior work. For fair comparison, we choose models sizes to be around 30M parameters, which are comparable to ours. They are summarized in [Table 3](#).
- *AllOffload*: The device offloads all inputs, for which the cloud runs a SOTA model [\[5\]](#): a two-pass end-to-end SLU model with one conformer-based encoder, one conformer-based deliberation encoder, two transformer-based decoders for the two passes, and a pretrained BERT language model. It has >10x parameters as compared to the local models above. We refer to its accuracy as *gold*.
- *NaiveHybrid*: To combine *OnDevice* and *AllOffload*, execute any input with probability α for local execution and $(1 - \alpha)$ for offloading.
- *Ours*: By varying the confidence threshold θ , we tested a range of variants which we refer to as *Ours-NoOffload* (0% offloaded), *Ours-Offload-L* (25%), *Ours-Offload-M* (47%), and *Ours-Offload-H* (63%).

7.2 End-to-end results

As demonstrated in Figure 4, XYZ is able to deliver a wide range of accuracies (from modest to nearly gold), with latencies as low as 100s of ms.

Compared to *OnDevice*, all variants of our system are better in the latency - accuracy trade-off. *Ours-Offload-M* and *Ours-Offload-H* achieve much higher accuracy (WER lower by 5%; IC higher by 2.5%) at similar or lower latencies; *Ours-NoOffload* achieves similar accuracies while reducing latencies by around 2x.

ASR

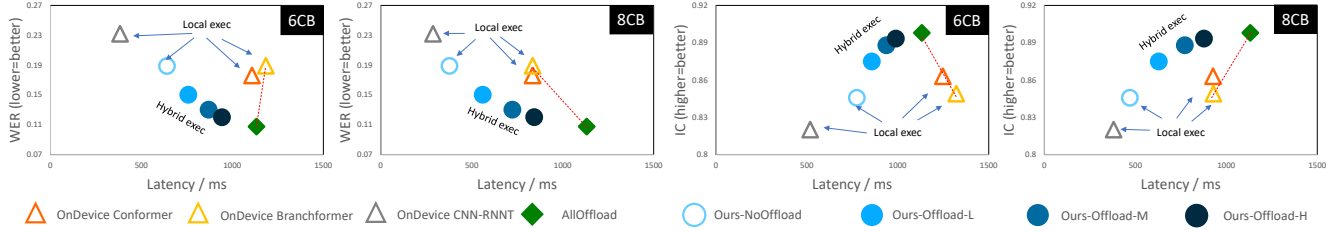


Figure 4: Our system deliver low delays and competitive accuracy. Compared to other local models (branchformer, conformer, CNN-RNN), our local execution (Ours-NoOffload) show similar accuracies at much lower delays; our hybrid executions show both better accuracies and delays. Compared to AllOffload, our hybrid executions show much lower delays with little accuracy loss.

	Conformer-M	Branchformer	CNN + RNN-T	Ours
Params	27.21M	36.02M	24.18M	23.33M
Encoder. embed	0.76G	3.02G	3.02G	3.02G
Encoder. encoders	0.01 (0.01)	0.04 (0.02)	0.03 (0.02)	0.03 (0.02)
Encoder. total	1.54G* (1.54G*)	1.88G* (1.88G*)	1.00G (0.34G*)	1.00G (0.34G*)
Decoder	2.30G (1.54G*)	4.90G (1.88G*)	4.02G	4.02G (0.34G*)
	0.11 (0.10*)	0.10 (0.09*)	0.17 (0.14*)	0.15 (0.12*)
				0.13 (0.02*)
				0.12 (0.02*)
				0.11 (0.02*)
				0.10 (0.02*)
				0.10* (0.02*)

Data labeled with * cannot be processed in streaming fashion.

Table 3: Our local encoder executes mostly streaming FLOPs, for which latency can be hidden behind IO; doing so does not compromise the final accuracy. FLOPs numbers normalized to 1 second of input. Our local execution path incur lower latencies (reported as RTF) for both encoding and decoding, as compared to other on-device models.

[fig: speedup ablation](#)

Compared to *AllOffload*, *Ours-Offload-L* and *Ours-Offload-M* reduce the overall latency by as much as 37% and 27% while seeing minor degradation in accuracy (no more than 4% WER and 2% of IC). They process 75% and 53% of inputs on device, reducing the need for cloud invocations by 2x or more. *Ours-Offload-H* has negligible accuracy degradation (<0.5% of IC) while still reducing latency by 20% and offload needs by 37%.

NaiveHybrid, shown as the dash lines interpolating between *OnDevice* and *AllOffload* on Figure 4, always shows inferior accuracy or latency to ours.

7.3 Efficacy of our local path

As shown in Figure 4, our local-only execution (*Ours-NoOffload*) significantly outperforms *OnDevice*, reducing latencies by 1.7x - 2.2x at similar accuracies. We next break down the benefit into two parts: encoding and decoding.

Encoding speedup We strike a sweet spot between speed (by processing inputs in a streaming fashion) and accuracy (by attending to the whole input). Table 3 breaks down the encoding computation.

Compared to encoders with all attention layers (Con/Branchformers) where 67% and 38% FLOPs are non-streaming (i.e. must execute *after* ingestion), 92% FLOPs of ours is streaming, for which the latency is hidden behind the ingestion IO. Meanwhile, we do not lose much accuracy compared to Con/Branchformers, as our design runs three attention layers after ingestion ends. This design

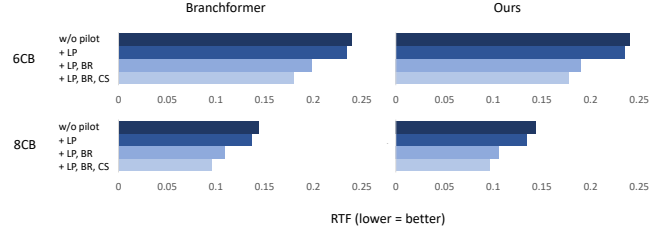


Figure 5: An ablation study of *pilot decoding*, showing that all its three optimizations contribute to lower latency significantly. It also shows that pilot decoding can apply to on-device models (e.g. Branchformer) other than ours. LP: length prediction, BR: Beam reduce, CS: CTC prefix scoring speedup

reduces the latency by 3.6x - 5.4x (220 - 345 ms or 0.07 - 0.11 RTF) as shown in Table 3.

Compared to full streaming encoders (CNN+RNN-T) for which 100% FLOPs is streaming, our accuracy is much higher by 4% in WER and 2.6% in IC, because the former critically lacks attention over the whole input. Meanwhile, our encoding latency is only higher by 0.005 RTF (15 ms for a typical 3 second input) as in Table 3. Such a difference is dwarfed by the difference in decoding delays.

Decoding speedup Our design shows 1.5x lower decoding delays compares to *OnDevice* (Table 3).

All three techniques show contribution to the overall speedup as Figure 5 shows. We also demonstrate the decoding speedup method on branchformer model. The speedup ratio is similar with it on ours model, shows that our speedup method is applicable on general transformer based encoder-decoder speech model.

The *incremental* nature of pilot decoding is crucial, as it amortizes the decoding cost over the past input, making the cost scale slower as the input grows. Turning off the incremental design (i.e. each pilot decoding starts from the input's start) increases the average decoding delay by 30%, from 156 ms to 205 ms; it increases the 90th percentile delay by 40%, from 198 ms to 282 ms. Reduction in pilot decoding cost makes our ingestion more efficient; it also allows to execute pilot decoding more frequently.

	NoOffload	Ours-Offload-L	Ours-Offload-H	
	RTF	RTF	Tgt / n Tgt	RTF
w/o pilot dec	0.168	0.238	1370 / 336	0.356
w/ pilot dec	$\tau=2s$	0.145	1743 / 932	0.298
	$\tau=1s$	0.138	1653 / 826	0.286
	$\tau=0.5s$	0.120	1644 / 657	0.268
			3534 / 2264	3534 / 2264

Table 4: Pilot decoding significantly reduces the end-to-end delay. It benefits our local-only execution (Ours-NoOffload) as well as our hybrid executions (Ours-Offload-X), for which the offloading are made more selective.

tab:psu

	WER=0.15		WER=0.14		WER=0.13		WER=0.12	
	RTF	offload	RTF	offload	RTF	offload	RTF	offload
NaiveHybrid	0.234	47.6%	0.264	59.8%	0.293	72.2%	0.323	84.5%
DeeBert	-	-	-	-	-	-	-	-
Ours	CNN	0.190	27.6%	0.215	37.8%	0.243	49.8%	0.280
	LSTM	0.171	21.5%	0.195	31.1%	0.222	43.0%	0.263
	PPL	0.178	25.0%	0.200	34.5%	0.230	47.3%	0.268
								65.7% offload
								60.2% offload

Table 5: Our offloading strategies based on sequence modeling outperform *NaiveHybrid* (random selection) and *DeeBERT* (sequence classification, failing to produce useful results). In the experiment, we tune θ and α to meet WER goals and compare delays and offloading ratio

ngstrategy

We further study the impact of pilot decoding’s eagerness: during ingestion, every τ seconds XYZ decodes the input it has accumulated so far. Lower τ reduces the discrepancy between the last pilot decoding and the full decoding, therefore improving the full decoding speed and quality. As shown in [Table 4](#), 4x reduction in τ (from 2s to 0.5 s) reduces final RTF by 0.025, further reduction in τ helps the pilot decoding get longer partial data that cover more part of the full length data. In exchange, the expense is that the ingestion consumes more compute. τ is lower bounded by the available compute bandwidth during ingestion. For instance, 8CB can sustain $\tau = 0.5s$ while 6CB cannot.

7.4 Efficacy of our offloading path

XYZ effectively identifies and uploads the inputs that would suffer from low accuracy on device.

Comparison vs. *NaiveHybrid* We replace XYZ’s offloading strategy with *NaiveHybrid* while keeping all other optimizations. The results in [Table 5](#) show that in order to reach the same accuracy (WER), *NaiveHybrid* has to offload up to 2x more inputs. The extra offloading translates to higher cloud cost as well as higher latency (additional 0.06 RTF; 180 ms on average).

[Figure 6](#) shows detailed offloading decisions: For *Ours-Offload-M* (WER=0.13) and *Ours-Offload-H* (WER=0.12), XYZ offloads the majority of target inputs, while still executing the majority of non-target inputs on device. This is much higher than *NaiveHybrid* which make decisions “by chance”.

Comparison vs. *DeeBERT* Our experiment also shows that a popular early-exit approach [36], estimating model confidence with linear classifiers inserted after each encoder transformer blocks, performs poorly for encoder-decoder SU models. We implemented such an approach: training linear classifiers atop the embedding of

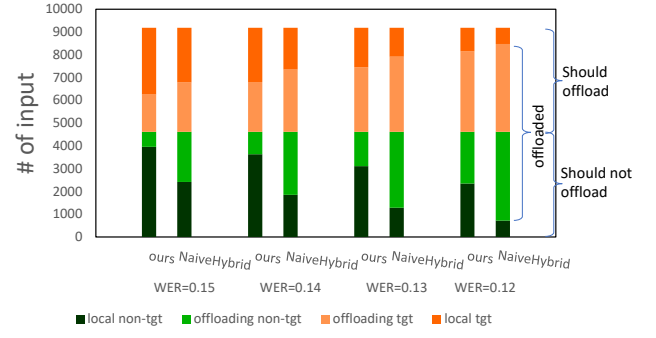


Figure 6: Our design shows good selectivity in making offloading decisions, offloading much fewer inputs compared to *NaiveHybrid* achieving similar accuracies.

the first output token at each layer. We could not get meaningful results – the classifier is no better than a random predictor. This highlights the challenge of predicting SU confidence, for which the entire generated sequence (not only just the input encoding) must be considered.

Choice of sequence modeling strategies The sequence modeling techniques in Section 6 (CNN, LSTM, and perplexity) can well estimate the model confidence. [Table 5](#) shows that LSTM offers the lowest offloading percentage and RTF. PPL perform slightly worse, but as perplexity has much lower computational complexity (no training, no parameters), we deem PPL as the most suitable.

How decoding affects offloading decisions? Recall that XYZ makes offloading decisions based on the last pilot decoding ([section 5](#)). We answer the following questions. (1) How does pilot decoding’s execution plan affect offloading decisions? Our results show that finer granularity (i.e. smaller discrepancy between the pilot and the full decoding) leads to better estimation of model confidence, which results in more accurate offloading decisions. For instance in [Table 4](#), to maintain the accuracy at WER=0.15, decreasing τ from 2 s to 0.5 s reduces the offloaded inputs by 14%, which translates to 93 ms lower end-to-end delay. (2) What if we make offloading decisions based on the *full* decoding outcome? Our results show that while the offloading selectivity slightly improves, the end-to-end latency is much higher (by 264 ms or 0.088 RTF), because the device makes offloading decisions much late – after ingesting the whole input and executing full decoding.

7.5 Sensitivity to system parameters

Device hardware and network delays (1) With faster device hardware, our local execution maintains consistent speed advantages over baselines, as shown by the comparison 6CB and 8CB, [Figure 4](#). This is because the pilot decoding speed up ratio maintains similar across different devices; besides, faster device computation can perform pilot decoding at higher rates. To extrapolate, if the device is so powerful that the decoding delay drops under the human perception threshold (around 50 ms), our advantage could become negligible. However, we do not expect that to happen soon, given

that today's speech models are increasingly larger and requiring more compute.

Our measurement was from decent network conditions (enterprise WiFi; 5G) that favor offloaded executions. With longer network delays, XYZ's benefit would be even more pronounced, as fast local executions and selective offloading will be more important. On the other hand, should network delays further reduce, the latency gap between our system and *OffloadAll* may narrow. Even if that happens, our benefit of reduced cloud cost will still remain.

Computation and Energy Efficiency Our system conserves computation when the input is relatively short. However, as the input length increases, the pilot decoding cost during ingestion may surpass the computation savings achieved during full decoding. In terms of energy costs, particularly on mobile devices, our system generally delivers energy savings. Mobile devices often exhibit high background energy consumption when not in sleep mode. Consequently, during ingestion, the pilot decoding may only result in a roughly 2x increase in energy costs. Nevertheless, the savings during full decoding are substantial with our system. If the system chooses to offload data to the cloud, the full decoding cost is reduced to 0. If local decoding is preferred, our speedup decoding can reduce the RTF by approximately 50%, leading to significant energy savings and enabling mobile devices to return to sleep mode earlier.

8 RELATED WORK

Comparing (PD) to speculative decoding (SD) First they address different challenges in different contexts. PD targets speech: the problem is temporal workload imbalance, during and after ingestion. SD targets LLM decoding (only the decoding phase): the problem is underutilized hardware parallelism (such as in server GPUs).

The solutions are different: PD decodes an *incomplete* input in order to extract helper information (beam search path, CTC scoring, sequence length); SD decodes a complete input, spawning fast and slow tasks concurrently. In particular, SD does not address speech because its decoding still expects full inputs and its speedup is contingent upon high hardware parallelism, which is lacking on an edge/embedded device.

The connection between the two is that the full decoding process benefit from an earlier decoding process (being a pilot or a speculative task).

ASR model design There are many works on ASR model designs. The state-of-the-art model designs can be divided into two lines: transducer-based streaming model and transformer-based end-to-end model. The transducer-based model, e.g. [10] [30] [40] process the data in a chunk-wise fashion which enable the streaming processing of the data. But at the same time, it only have monotonic partial data information during the streaming processing, thus compromise the accuracy. The transformer-based model, e.g. [6] [11] [27] process the complete data with all-to-all attention-based encoder-decoder model, which fully exploit the context information and reach the state-of-the-art accuracy. Our work focus on transformer-based model processing optimization, largely reduces the latency while maintains the accuracy.

Speculative decoding There is a line of work focusing on decoding speedup, also called "aggressive decoding". The key is to

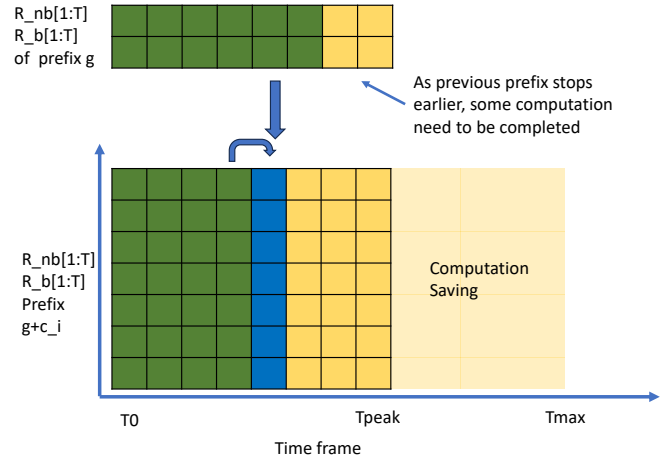


Figure 7: Truncate CTC algorithm in Online hybrid CTC/Attention. Base on the peaky CTC assumption, the algorithm discard part of the computation on later time frame after the CTC peak

address the efficiency bottleneck in sequential decoding (autoregression). For example, [37] finds that the decoding results usually have identical part with the input. The authors thus propose a novel decoding scheme. During the decoding, the system copy a span of input tokens to the output during the autoregressive decoding. Then verify if these copied tokens are indeed the expected decoded tokens. Verification of individual tokens can be done in parallel, which better utilize the hardware parallelism. [35] adopt non-autoregressive translation method to first generate draft, then use decoder to perform verification on the draft. Both process can be done in parallel. [33] focus on Grammar Error Correction task. They adopt shallow decoder and parallel decoding method. There is also a verification step, which will most likely succeed due to the nature of the task. [16] use two decoders in decoding, small decoder for most of the token, while big decoder for some difficult ones. The authors also designed fall back and roll back mechanisms to help further improve the overall accuracy of the model. The above methods generally try to first generate tentative results with light weight / parallel methods and then verify the results. But all of them are working on nlp related tasks. Speech processing is quite different: it does not have text input as inference, the data representation is different, and it has long ingestion time. Our method take use of it and generate tentative results from partial input. Then use verification to help mitigate the beam search latency overhead.

Offloading and hybrid execution There are series of work working on device-cloud collaboration. [38] focus on efficient offloading, proposes method to compress the data to reduce the offloading overhead in bandwidth-limited scenarios. [22] proposes a large-scale production system for device-cloud collaboration. It contains local containers and VM for local execution optimization and data pipeline for low latency device-cloud communication. Different from the above two works, our system selectively offload the data, and make the decision before the data is complete in streaming scenarios.

Comparing CTC Leap with the Online CTC/Attention Method

Both methods target speech tasks but operate at different processing stages, offering distinct solutions to accelerate CTC prefix scoring. The Online CTC/Attention method, including the Truncated CTC prefix scoring (T-CTC) method, focuses on processing streaming data in real-time (but we have full length data for full decoding). During the scoring of a specific prefix, the T-CTC method only has access to partial streaming data. Leveraging the nature of CTC, T-CTC employs a dynamic programming algorithm but aims to identify the CTC peak corresponding to the last token in the prefix, estimating the $p_{ctc}(h|T)$ by $p_{ctc}(h|T_{token})$.

In more detail, the T-CTC method based on the assumption that CTC posterior probability shows peaky pattern. For each token in the transcript, only one corresponding time frame will show high CTC posterior probability for that token. For most of the time frame all the tokens have evenly low CTC posterior probability. The original hybrid CTC/Attention algorithm does not take any assumption on prefix - time frame alignment, and calculate each prefix through a dynamic programming algorithm among all the time frames from T_0 to T_{max} . But with the peaky assumption in T-CTC algorithm, the dynamic programming algorithm only need to calculate from the beginning time frame to the corresponding time frame that show large probability on the new (latest) token in the prefix, i.e. from T_0 to T_{token} . Although to calculate new prefix probability we need to still proceed the previous prefix's calculation forward, most of the prefix will be discarded in the beam search process and enjoy the calculation saving.

In contrast, CTC Leap in our system operates with full-length data. It ensures the dynamic programming algorithm considers all time frames but skips the earlier part of the time frames that have already been calculated (or at least have similar calculations done) during pilot inference. The commonality between the two methods lies in their attempt to skip part of the CTC prefix scoring computation. However, our method achieves this without discarding temporal information.

9 CONCLUDING REMARKS

We present XYZ, a novel system for fast speech processing tasks. XYZ contributes late contextualization, beam collapse, beam search early termination and ctc leap techniques for local execution and confidence estimation techniques for hybrid execution collaborating with cloud service. The former allows XYZ accelerate local execution while the latter one enables users to better trade-off the accuracy and latency. With the techniques the XYZ can reduce 2x for local execution, and reduce 50% or more offloading and cloud service queries for hybrid execution.

REFERENCES

- [1] Azure hybrid benefit, 2023. Accessed: 2023-11-18.
- [2] Azure-samples/cognitive-services-speech-sdk, 2023. Accessed: 2023-01-24 speech
- [3] The future of ai is hybrid, 2023. Accessed: 2023-11-18.
- [4] Generative ai trends by the numbers: Costs, resources, parameters and more, 2023. Accessed: 2023-7-26.
- [5] Siddhant Arora, Siddharth Dalmia, Xuankai Chang, Brian Yang, Alan Black, and Shinji Watanabe. Two-pass low latency end-to-end spoken language understanding. In *Proceedings of the Annual Conference of the International Speech Communication Association, INTERSPEECH*, volume 2022, pages 3478–3482, 2022.
- [6] Alexei Baevski, Yuhao Zhou, Abdelrahman Mohamed, and Michael Auli. wav2vec 2.0: A framework for self-supervised learning of speech representations. *Advances in neural information processing systems*, 33:12449–12460, 2020.
- [7] Emanuele Bastianelli, Andrea Vanzo, Paweł Swietojanski, and Verena Rieser. SLURP: A Spoken Language Understanding Resource Package. In *Proceedings of the 2020 Conference on Empirical Methods in Natural Language Processing (EMNLP)*, 2020.
- [8] Jan K Chorowski, Dzmitry Bahdanau, Dmitriy Serdyuk, Kyunghyun Cho, and Yoshua Bengio. Attention-based models for speech recognition. In C. Cortes, N. Lawrence, D. Lee, M. Sugiyama, and R. Garnett, editors, *Advances in Neural Information Processing Systems*, volume 28. Curran Associates, Inc., 2015.
- [9] Renato De Mori. Spoken language understanding: A survey. In *2007 IEEE Workshop on Automatic Speech Recognition & Understanding (ASRU)*, pages 365–376. IEEE, 2007.
- [10] Alex Graves. Sequence transduction with recurrent neural networks. *arXiv preprint arXiv:1211.3711*, 2012.
- [11] Anmol Gulati, James Qin, Chung-Cheng Chiu, Niki Parmar, Yu Zhang, Jiahui Yu, Wei Han, Shibo Wang, Zhengdong Zhang, Yonghui Wu, and Ruoming Pang. Conformer: Convolution-augmented transformer for speech recognition. *CoRR*, abs/2005.08100, 2020.
- [12] Awni Y. Hannun. The history of speech recognition to the year 2030. *ArXiv*, abs/2108.00084, 2021.
- [13] Wei-Ning Hsu, Benjamin Bolte, Yao-Hung Hubert Tsai, Kushal Lakhotia, Ruslan Salakhutdinov, and Abdelrahman Mohamed. Hubert: Self-supervised speech representation learning by masked prediction of hidden units. *IEEE/ACM Trans. Audio, Speech and Lang. Proc.*, 29:3451–3460, oct 2021.
- [14] Frederick Jelinek, Robert L. Mercer, Lalit R. Bahl, and Janet M. Baker. Perplexity—a measure of the difficulty of speech recognition tasks. *Journal of the Acoustical Society of America*, 62, 1977.
- [15] Jungo Kasai, Keisuke Sakaguchi, Ronan Le Bras, Dragomir Radev, Yejin Choi, and Noah A. Smith. Beam decoding with controlled patience, 2022.
- [16] Sehoon Kim, Karttikaya Mangalam, Suhong Moon, John Cann, Jitendra Malik, Michael W. Mahoney, Amir Gholami, and Kurt Keutzer. Speculative decoding with big little decoder. In *Advances in Neural Information Processing Systems*. Curran Associates, Inc., 2023.
- [17] Hong-Kwang J Kuo, Zoltán Tüske, Samuel Thomas, Yinghui Huang, Kartik Audhkhasi, Brian Kingsbury, Gakufo Kurata, Zvi Kons, Ron Hoory, and Luis Lastra. End-to-end spoken language understanding without full transcripts. In *INTERSPEECH*, 2020.
- [18] Niel Lebeck, Arvind Krishnamurthy, Henry M. Levy, and Irene Zhang. End the senseless killing: Improving memory management for mobile operating systems. In *2020 USENIX Annual Technical Conference (USENIX ATC 20)*, pages 873–887. USENIX Association, July 2020.
- [19] Sooyon Lee and Hyokyung Bahn. Characterization of android memory references and implication to hybrid memory management. *IEEE Access*, 9:60997–61009, 2021.
- [20] Jinyu Li, Yu Wu, Yashesh Gaur, Chengyi Wang, Rui Zhao, and Shujie Liu. On the comparison of popular end-to-end models for large scale speech recognition. In Helen Meng, Bo Xu, and Thomas Fang Zheng, editors, *Interspeech 2020, 21st Annual Conference of the International Speech Communication Association, Virtual Event, Shanghai, China, 25–29 October 2020*, pages 1–5. ISCA, 2020.
- [21] Baiyang Liu, Björn Hoffmeister, and Ariya Rastrow. Accurate endpointing with expected pause duration. In *Interspeech*, 2015.
- [22] Chengfei Lv, Chaoyue Niu, Renjie Gu, Xiaotang Jiang, Zhaode Wang, Bin Liu, Ziqi Wu, Qiulin Yao, Congyu Huang, Panos Huang, et al. Walle: An {End-to-End}, {General-Purpose}, and {Large-Scale} production system for {Device-Cloud} collaborative machine learning. In *16th USENIX Symposium on Operating Systems Design and Implementation (OSDI 22)*, pages 249–265, 2022.
- [23] Sumit Maheshwari, Dipankar Raychaudhuri, Ivan Seskar, and Francesco Bronzino. Scalability and performance evaluation of edge cloud systems for latency constrained applications. In *2018 IEEE/ACM Symposium on Edge Computing (SEC)*, pages 286–299, 2018.
- [24] A. Martin, D. Charlet, and L. Mauuary. Robust speech/non-speech detection using lda applied to mfcc. In *2001 IEEE International Conference on Acoustics, Speech, and Signal Processing. Proceedings (Cat. No.01CH37221)*, volume 1, pages 237–240 vol.1, 2001.
- [25] Haoran Miao, Gaofeng Cheng, Pengyuan Zhang, and Yonghong Yan. Online hybrid ctc/attention end-to-end automatic speech recognition architecture. *IEEE/ACM Transactions on Audio, Speech, and Language Processing*, 28:1452–1465, 2020.
- [26] Vassil Panayotov, Guoguo Chen, Daniel Povey, and Sanjeev Khudanpur. Librispeech: An asr corpus based on public domain audio books. In *2015 IEEE International Conference on Acoustics, Speech and Signal Processing (ICASSP)*, pages 5206–5210, 2015.
- [27] Yifan Peng, Siddharth Dalmia, Ian Lane, and Shinji Watanabe. Branchformer: Parallel mlp-attention architectures to capture local and global context for speech recognition and understanding. In *International Conference on Machine Learning*, pages 17627–17643. PMLR, 2022.

deepcontext
radford23a
exploring
2019spoken
2020survey
tantaneous
7hybridctc

[28] Golan Pundak, Tara N. Sainath, Rohit Prabhavalkar, Anjuli Kaman, and Dileep Zhao. Deep context: End-to-end contextual speech recognition. In *2018 IEEE Spoken Language Technology Workshop (SLT)*, pages 418–425, 2018.

[29] Alec Radford, Jong Wook Kim, Tao Xu, Greg Brockman, Christine Metzger, and Ilya Sutskever. Robust speech recognition via large-scale weak supervision. In Andreas Krause, Emma Brunskill, Kyunghyun Cho, Barbara Engelhardt, Sivan Sabato, and Jonathan Scarlett, editors, *Proceedings of the 40th International Conference on Machine Learning*, volume 202 of *Proceedings of Machine Learning Research*, pages 28492–28518. PMLR, 23–29 Jul 2023.

[30] Kanishka Rao, Haşim Sak, and Rohit Prabhavalkar. Exploring architectures, data and units for streaming end-to-end speech recognition with rnntransducer. In *2017 IEEE Automatic Speech Recognition and Understanding Workshop (ASRU)*, pages 193–199. IEEE, 2017.

[31] Alaa Saade, Joseph Dureau, David Leroy, Francesco Caltagirone, Alice Coucke, Adrien Ball, Clément Doumouro, Thibaut Lavril, Alexandre Caulier, Théodore Bluché, et al. Spoken language understanding on the edge. In *2019 IEEE Workshop on Energy Efficient Machine Learning and Cognitive Computing Near the Edge (EMC2-NIPS)*, pages 57–61. IEEE, 2019.

[32] Ali Shakarami, Mostafa Ghobaei-Arani, and Ali Shahidinejad. A survey on the computation offloading approaches in mobile edge computing: A machine learning-based perspective. *Computer Networks*, 182:107496, 2020.

[33] Xin Sun, Tao Ge, Furu Wei, and Houfeng Wang. Instantaneous grammatical error correction with shallow aggressive decoding. *arXiv preprint arXiv:2106.04970*, 2021.

[34] Shinji Watanabe, Takaaki Hori, Suyoun Kim, John R. Hershey, and Tomoki Hayashi. Hybrid ctc/attention architecture for end-to-end speech recognition. *IEEE Journal of Selected Topics in Signal Processing*, 11(8):1240–1253, 2017.

[35] Heming Xia, Tao Ge, Furu Wei, and Zhifang Sui. Lossless speedup of autoregressive translation with generalized aggressive decoding. *arXiv preprint arXiv:2203.16487*, 2022.

[36] Ji Xin, Raphael Tang, Jaejun Lee, Yaoliang Yu, and Jimmy Lin. DeeBERT: Dynamic early exiting for accelerating BERT inference. In *Proceedings of the 58th Annual Meeting of the Association for Computational Linguistics*, pages 2246–2251, Online, July 2020. Association for Computational Linguistics.

[37] Nan Yang, Tao Ge, Liang Wang, Binxing Jiao, Dixin Jiang, Linjun Yang, Rangan Majumder, and Furu Wei. Inference with reference: Lossless acceleration of large language models. *arXiv preprint arXiv:2304.04487*, 2023.

[38] Shuochao Yao, Jinyang Li, Dongxin Liu, Tianshi Wang, Shengzhong Liu, Huajie Shao, and Tarek Abdelzaher. Deep compressive offloading: Speeding up neural network inference by trading edge computation for network latency. In *Proceedings of the 18th Conference on Embedded Networked Sensor Systems*, SenSys '20, page 476–488, New York, NY, USA, 2020. Association for Computing Machinery.

[39] Dong Yu and Lin Deng. *Automatic speech recognition*, volume 1. Springer, 2016.

[40] Qian Zhang, Han Lu, Hasim Sak, Anshuman Tripathi, Erik McDermott, Stephen Koo, and Shankar Kumar. Transformer transducer: A streamable speech recognition model with transformer encoders and rnnt loss. In *ICASSP 2020–2020 IEEE International Conference on Acoustics, Speech and Signal Processing (ICASSP)*, pages 7829–7833. IEEE, 2020.

[41] Wangchunshu Zhou, Canwen Xu, Tao Ge, Julian McAuley, Ke Xu, and Furu Wei. Bert loses patience: Fast and robust inference with early exit. In H. Larochelle, M. Ranzato, R. Hadsell, M.F. Balcan, and H. Lin, editors, *Advances in Neural Information Processing Systems*, volume 33, pages 18330–18341. Curran Associates, Inc., 2020.